

# Electron Spin Polarization after Photolysis of AIBN in Solution: Initial Spatial Radical Separation

Anton N. Savitsky and Henning Paul\*

Physical-Chemistry Institute, University of Zurich, CH-8057 Zurich, Switzerland

Anatoly I. Shushin

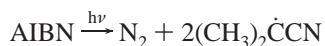
Institute of Chemical Physics, RAS, GSP-1, 117977 Moscow, Russia

Received: May 23, 2000; In Final Form: July 20, 2000

Transient 2-cyano-2-propyl radicals are generated by laser flash photolysis of 2,2'-azobisisobutyronitrile (AIBN) in solvents of various viscosities. Their spin magnetization is followed by time-resolved EPR spectroscopy and analyzed in terms of modified Bloch equations accounting for chemical reaction, Heisenberg spin exchange, and rise and decay of chemically induced electron polarization (CIDEP). The results are: (i) The cross-section for spin exchange exceeds that for radical termination by a factor of 1.8. (ii) No geminate net polarization is found, implying that eventually formed primary diazenyl radicals decay on the picosecond time scale. (iii) The ratio of F-pair and geminate pair polarization increases with viscosity from  $|P_F/P_G| = 1$  at  $\eta = 0.6$  cP to  $|P_F/P_G| = 4.7$  at  $\eta = 18$  cP. According to the diffusion theory of CIDEP, this means that the initial spatial distance  $r_i$  of the radicals escaping the geminate cage is independent of the viscosity. This finding is at variance with the cage effect, which is predicted correctly by classical Langevin models assuming a decrease of  $r_i$  with increasing viscosity. It is tentatively concluded that, at least for AIBN, the successful simulation of the  $\eta$ -dependent cage effect is only fortuitous and conceptually wrong.

## 1. Introduction

2,2'-Azobisisobutyronitrile (AIBN) is one of the most extensively studied azoalkanes because of its use as a polymerization initiator.<sup>1,2</sup> Upon UV excitation it decomposes into a nitrogen molecule and a geminate pair (G-pair) of two 2-cyano-2-propyl radicals,



As the cleavage occurs from the singlet state, a considerable portion of the G-pairs decays rapidly by radical termination to form in-cage recombination and disproportionation products. Those species, which escape the cage effect, diffuse apart, form F-pairs by subsequent random diffusive encounters, and terminate if they happen to encounter in a singlet-pair spin state.

The radicals escaping the G- and F-pairs are detectable by time-resolved EPR (TREPR) spectroscopy. They exhibit chemically induced electron polarization (CIDEP), that is, the populations of their spin states deviate from thermal equilibrium. This phenomenon is caused by the radical pair mechanism (RPM) and arises during re-encounter sequences of the spin-correlated G- and F-pairs via mixing and splitting of the singlet- and triplet-pair spin states by the hyperfine and exchange interaction, respectively. The polarization causes the low-field EPR transitions to appear in emission (E) and the high-field ones in enhanced absorption (A), or vice versa. Whether an E/A or A/E multiplet pattern is produced depends on the sign of the exchange interaction and the spin state multiplicity of the pairs when formed. The magnitude of the polarization is determined by the distance dependence of the exchange interaction  $J(r)$  between the radicals of the pair, their hyperfine splitting, their

relative diffusion coefficient  $D$ , and the initial radical separation when the pair is generated.<sup>3–5</sup>

The G- and F-pairs after photolysis of AIBN are both composed of two 2-cyano-2-propyl radicals. With respect to the RPM, the essential difference between both pairs is only the initial spatial distance, in which the radicals start their diffusive trajectories of the re-encounter process, along which the CIDEP is generated. For the F-pairs, this initial separation should be the distance of closest approach of the species. There, the pair system is prepared in its triplet state, because the singlet pairs are filtered out by radical termination. For the G-pairs, the initial distance  $r_i$  is not well-known. After photodissociation of a molecule in solution there seems to be a fairly short primary separation stage of the fragments, which is accompanied by fast vibrational and translational relaxation.<sup>6,7</sup> After dissipation of the initial energy, the radicals that have escaped fast recombination during the primary separation stage will have a certain distribution of initial distances  $r_i$ , the average of which may be estimated from a Langevin model, for example. The primary separation stage occurs on the early picosecond time scale, which is much shorter than the time needed for spin evolution (typically nanoseconds) and, with it, the generation of CIDEP. Therefore, the RPM spin polarization of the G-pairs depends on only the average initial distance  $r_i$ .

In this article we report on quantitative measurements of the spin polarizations, which are generated in the G- and F-pairs after photolysis of AIBN in solvents of different viscosity. Because all details concerning the diffusion and the distance dependence of the exchange interaction are the same for both pairs, the polarization ratio  $|P_F/P_G|$  should provide a reliable look at the viscosity dependence of  $r_i$ , allowing verification of the quality of common Langevin models. For the solvents used

we have also determined the cage effect, which should be composed of a “primary” and “secondary” cage effect.<sup>8</sup> The primary cage effect occurs on the femto- to picosecond time scale during separation of the fragments and has no direct connection with  $r_i$ . The secondary one, however, is determined by the probability for diffusive return of the radicals from  $r_i$  to the reaction distance, and any meaningful model for the viscosity dependence of  $r_i$  must be able to reproduce the viscosity dependence of both the secondary cage effect and the ratio of spin polarizations  $|P_F/P_G|$ .

## 2. Experimental Section

Our experimental arrangement for TREPR measurements after laser flash photolytic radical initiation has been described in detail previously.<sup>9</sup> For the AIBN studies we used a frequency tripled Nd:YAG laser (355 nm, 6-ns pulse length, 10-Hz repetition rate, 1–15 mJ per pulse on sample surface). Solutions containing AIBN (74 mM) were deoxygenated by bubbling with Ar for 45–60 min and pumped in continuous flow (flow rate  $5.55 \mu\text{L}\cdot\text{s}^{-1}$ ) through a flat quartz cell (2-mm optical path) inside the TE103 EPR cavity. The depletion of AIBN was controlled by optical absorption spectroscopy and kept at less than 15%. All experiments were performed at 293 K.

The solvents were chosen according to the solubility of AIBN and covered a wide range of viscosities. We used benzene, ethyl benzoate (EB), di-*n*-butyl phthalate (BP), and their volume mixtures: mix A (benzene/BP, 40/60), mix B (benzene/BP, 26/74), mix I (EB/BP, 50/50), and mix II (EB/BP, 20/80). The product distribution was checked by NMR and gas chromatography for all solvents. Ninety-two percent combination products [tetramethylsuccinodinitrile and dimethyl-*N*-(2-cyano-2-propyl)-ketenimine] and 8% disproportionation products (isobutyronitrile and methacrylonitrile) were found, varying only a little with solvent and temperature, in agreement with earlier studies of the thermolysis and photolysis of AIBN.<sup>10</sup> The product distribution is stable to irradiation at 355 nm. (Noticeable product absorption, mainly due to the ketenimine, starts at less than 340 nm.)

Also the chemical kinetics of 2-cyano-2-propyl radicals generated by UV irradiation of AIBN in all the solvents used was checked in kinetic EPR experiments, using a setup that has been described elsewhere.<sup>11</sup> The investigations gave clean second-order decay profiles for 2-cyano-2-propyl radicals in solvents of high viscosity (ethyl benzoate and dibutyl phthalate) at temperatures between 290 and 320 K. Contaminations by unknown pseudo-first-order radical reactions were always less than 3%. Photolysis of AIBN in benzene led to a similarly clean kinetic behavior of the EPR signals only for temperatures above 310 K. At lower temperatures the time profiles were distorted by an unknown slow decay kinetics in a way similar to that reported previously.<sup>12</sup> However, no indications for this slow decay were found in the TREPR experiments after laser flash photolysis of AIBN under these conditions. The self-termination of the radicals seems to remain the dominant reaction on the time scale of the TREPR experiment, probably because the initial radical concentration after laser flash photolysis is about 2 orders of magnitude larger than in the kinetic EPR experiments.

The viscosities of the sample solutions were determined using calibrated Ubbelohde capillary viscometers. Diffusion coefficients of the radicals in the solution were measured by a chromatographic broadening technique<sup>13a</sup> using isobutyronitrile to model the 2-cyano-2-propyl radicals.<sup>13b</sup> Chemicals were purchased from Fluka, Aldrich, and SDS in their purest commercially available forms and used as supplied.

## 3. Analysis of EPR-Time Profiles

The EPR-time profiles that are obtained after flash photolytic radical initiation contain all information about the chemical and spin dynamics of the system. They were analyzed on the basis of Bloch equations, modified with additional terms to allow for chemical kinetics, CIDEP, and Heisenberg spin exchange. The modification and the procedure of analysis are outlined below.

Considering a system of identical radicals with certain nuclear spin states, we denote as  $N_i (N_\alpha^i + N_\beta^i)$  the number of radicals occupying the nuclear spin state  $i$ , and as  $n_i (N_\alpha^i - N_\beta^i)$  the population difference in that hyperfine state. In the absence of chemical reaction,  $N_i$  will be constant, and any initial population difference  $n_i$  will change according to the rate law

$$\frac{d}{dt}n_i = -\frac{1}{T_1}[n_i - p_{\text{eq}}N_i] - k_{\text{ex}}\left[n_i\sum_j N_j - N_i\sum_j n_j\right] \quad (3.1)$$

The first term on the right-hand side describes the spin-lattice relaxation of  $n_i$  to its thermal equilibrium value  $p_{\text{eq}}N_i$ , with  $p_{\text{eq}} = g\mu_B B_0 / (2kT)$ . The second term takes into account the loss and gain of  $n_i$  as a result of Heisenberg spin exchange.<sup>14–17</sup>

If the radicals react by bimolecular termination the decay of  $N_i$  should follow the rate law

$$\frac{d}{dt}N_i = -\left[N_i\sum_j k_2 N_j - n_i\sum_j k_2 n_j\right] \quad (3.2)$$

Relation 3.2 is based on the assumption that only those radicals that form singlet radical pairs upon collision can terminate. If the electron spin system is only weakly polarized, that is,  $n_{i,j} \ll N_{i,j}$ , or carries only a multiplet type polarization,  $\sum_j n_j \approx p_{\text{eq}}N$ , the second term on the right-hand side is negligible and the decay of  $N_i$  is governed by the first one, the usual second-order rate law. However, if the spin system exhibits a strong net polarization, the second term might become important, because it corrects for the surplus of  $\alpha$ - or  $\beta$ -spins. (In the limiting case of a completely net polarized electron spin system with only  $\alpha$ - or  $\beta$ -spins, the second term would cancel the first one, thus preventing any termination.)

For systems of reactive radicals rate law 3.1 for the population difference has to be changed to account for the generation of F-pair CIDEP. F-pairs are formed by diffusion-controlled encounters of radicals. The probabilities for encountering initially as T<sub>0</sub>- or S-state radical pair are the same. According to the RPM the spin polarizations developed in T<sub>0</sub>- and S-state pairs are of equal magnitude but opposite sign. Thus, in the absence of any spin state selective radical termination the CIDEP stemming from T<sub>0</sub> and S encounters would cancel each other. However, if singlet F-pairs are partially or completely filtered out by radical termination, as is usually the case, the CIDEP from the T<sub>0</sub> encounters will dominate and change the population difference  $n_i$ . Because there are as many excess T<sub>0</sub> pairs as S pairs that have reacted, the necessary modification of eq 3.1 immediately follows from eq 3.2 and is given by

$$\frac{d}{dt}n_i = -\frac{1}{T_1}[n_i - p_{\text{eq}}N_i] - k_{\text{ex}}\left[n_i\sum_j N_j - N_i\sum_j n_j\right] + N_i\sum_j k_2 p_{\text{F}}(i,j)N_j - n_i\sum_j k_2 p_{\text{F}}(i,j)n_j \quad (3.3)$$

As a consequence of the RPM, the rate constant  $k_2$  for bimolecular radical termination depends on the hyperfine states

$i$  and  $j$  as well. This dependence can be estimated from<sup>18</sup>

$$k_2(i,j) = \frac{1 + \sqrt{Q(i,j) \cdot d^2/D}}{1 + \sqrt{1/2} \sqrt{Q(i,j) \cdot d^2/D}} \cdot k_2 \quad (3.4)$$

where  $D$  is the relative diffusion coefficient of the radicals forming the pair,  $d$  is their distance of closest approach,  $Q(i,j)$  is half the difference of their Lamor frequencies, and  $k_2$  is the termination rate constant for  $Q(i,j) = 0$  (i.e., no T<sub>0</sub>-S mixing). However, in most cases this dependence is weak enough to be negligible, and the nuclear spin polarization in the radicals also can be neglected as long as eq 3.4 yields  $k_2(i,j) \approx k_2$ . Given this condition, the population of the hyperfine state  $i$  is  $N_i = x_i N/x$ , where  $x$  is the number of nuclear spin states and  $x_i$  is the degeneracy of the  $i$ th state. Denoting the total number of radicals with  $N = \sum N_j$ , the total population difference with  $n = \sum n_j$ , and neglecting the usually tiny last terms on the right-hand side of eqs 3.2 and 3.3, these relations give

$$\frac{d}{dt} n_i = -\frac{1}{T_1} [n_i - p_{\text{eq}} N_i] - k_{\text{ex}} [n_i N - n N_i] + k_2 N N_i p_{\text{F}}(i) \quad (3.5)$$

$$\frac{d}{dt} n = -\frac{1}{T_1} [n - p_{\text{eq}} N] + k_2 N^2 \sum_i \frac{x_i}{x} \cdot p_{\text{F}}(i) \quad (3.6)$$

$$\frac{d}{dt} N = -k_2 N^2 \quad (3.7)$$

where

$$p_{\text{F}}(i) = \sum_j \frac{x_j}{x} \cdot p_{\text{F}}(i,j) \quad (3.8)$$

Equation 3.6 contains the additional assumption that the spin-lattice relaxation time  $T_1$  does not depend on the nuclear spin states. This holds only for small radicals in low viscous solution, when their relaxation is dominated by spin-rotation interaction.

For identical radicals the RPM generates a pure multiplet CIDEP (usually E/A for F-pairs). Thus, the second term in eq 3.6 is zero. Transformation to magnetizations then yields

$$\frac{d}{dt} M_Z = -\frac{1}{T_1} [M_Z - P_{\text{eq}}[R]] - k_{\text{ex}}[R] [M_Z - M_Z^{\text{tot}}] + 2k_t[R]^2 P_{\text{F}} P_{\text{eq}} \quad (3.9)$$

$$\frac{d}{dt} M_Z^{\text{tot}} = -\frac{1}{T_1} [M_Z^{\text{tot}} - P_{\text{eq}}[R]] \quad (3.10)$$

$$\frac{d}{dt} [R] = -2k_t[R]^2 \quad (3.11)$$

where  $M_Z$  is now the  $z$ -magnetization of the radicals in the nuclear spin state  $i$ , which are assumed to be the ones under EPR investigation. They relax to an equilibrium value  $P_{\text{eq}}[R]$  with  $P_{\text{eq}} = 1/2 g \mu_{\text{B}} p_{\text{eq}} N_{\text{A}} x_i/x$  and  $[R]$  being the radical concentration in mol/dm<sup>3</sup> ( $N_{\text{A}}$  = Avogadro's number).  $M_Z^{\text{tot}} = 1/2 g \mu_{\text{B}} n x_i/x$  is the total  $z$ -magnetization of the electron ensemble, normalized to the transition under EPR investigation,  $2k_t$  denotes the rate constant for termination (in M<sup>-1</sup>·s<sup>-1</sup>), and  $P_{\text{F}}$  is the F-pair polarization, defined as  $P_{\text{F}} = p_{\text{F}}(i)/p_{\text{eq}}$ .

To describe the time dependence of the magnetization by Bloch equations, it is assumed that the microwave field interacts only with radicals in a certain defined hyperfine state. Interactions of the B<sub>1</sub>-field with species in the other hyperfine states have to be negligibly small, that is, neighboring resonances must be well separated with negligible overlap. Taking into account that the polarization processes lead to changes of the  $z$ -magnetization only, whereas the exchange affects all components of the magnetization, the Bloch equations may be written as

$$\frac{d}{dt} u = -\frac{u}{T_2^{\text{eff}}} - \Delta \omega \cdot v$$

$$\frac{d}{dt} v = \Delta \omega \cdot u - \frac{v}{T_2^{\text{eff}}} + \omega_1 M_z \quad (3.12)$$

$$\frac{d}{dt} M_z = -\omega_1 v - \frac{M_z}{T_1^{\text{eff}}} + f_{\text{a}}(t)$$

with

$$\frac{1}{T_{1,2}^{\text{eff}}} = \frac{1}{T_{1,2}} + k_{\text{ex}}[R] \quad (3.13)$$

and

$$f_{\text{a}}(t) = \frac{1}{T_1} \cdot P_{\text{eq}}[R] + k_{\text{ex}}[R] M_z^{\text{tot}} + 2k_t[R]^2 P_{\text{F}} P_{\text{eq}} \quad (3.14)$$

In eq 3.12 the impact of the exchange on the perpendicular magnetizations  $u$  and  $v$  is accounted for only as an additional loss rate  $k_{\text{ex}}[R]$  besides the relaxation rate  $1/T_2$ , that is, it is assumed that the expectation values of the perpendicular components of the total magnetization are solely determined by  $u$  and  $v$  of the EPR line under resonance. For this assumption to be a good approximation it not only requires that the B<sub>1</sub>-field does not interact with other EPR lines, but also that the line under resonance has only a small statistical weight, that is,  $x_i/x \ll 1$ .

As a whole, for a system of identical radicals the dependence on time of an EPR line  $i$  should be describable by relations 3.10–3.14 under the following conditions:

1. The reactivity of the radicals is independent of their hyperfine state.
2. The radicals populate their hyperfine states according to their degeneracies, that is,  $N_j = x_j N/x$ .
3. The line under study has only a small statistical weight, that is,  $x_i/x \ll 1$ .
4. The termination rate of the radicals is slower than the spin-lattice relaxation rate.
5. The spin polarization of the radicals does not contain a large net polarization. The AIBN system was checked carefully under the conditions of its investigation and met all these requirements in sufficient approximation.

The generation of the spin-polarized radicals occurs on time scales that are much shorter than that of the TREPR experiment and, therefore, enters as initial condition, that is,

$$[R](0) = [R]_0 \quad (3.15)$$

$$M_z(0) = (P_n + P_m) P_{\text{eq}}[R]_0 \quad (3.16)$$

$$M_z^{\text{tot}}(0) = P_n P_{\text{eq}}[R]_0 \quad (3.17)$$

where  $P_n$  and  $P_m$  are the potential initial net and multiplet

polarizations, respectively. The initial perpendicular magnetizations are always set  $u = v = 0$ .

In the absence of exchange, that is, if  $T_{1,2}k_{\text{ex}}[R]_0 \ll 1$ , the time dependence of an initial magnetization  $M_Z(0)$  is given by eq 3.12, with relaxation times  $T_{1,2}^{\text{eff}} = T_{1,2}$  and  $f_a(t)$  [and therefore also  $M_Z(t)$ ] being independent of  $M_Z^{\text{tot}}(t)$ . Then, the time dependence of the  $v$ -magnetization under resonance conditions is simply given by

$$v(t) = \frac{\omega_1}{\omega_T} \cdot M_Z(0) \cdot e^{-\sigma_0 t} \cdot \sin \omega_T t + \frac{\omega_1}{\omega_T} \cdot f_a'(t) \otimes (e^{-\sigma_0 t} \cdot \sin \omega_T t) \quad (3.18)$$

with

$$\sigma_0 = 1/2 \left( \frac{1}{T_1} + \frac{1}{T_2} \right), \quad \text{and} \quad \omega_T = \sqrt{\omega_1^2 - \frac{1}{4} \left( \frac{1}{T_1} - \frac{1}{T_2} \right)^2} \quad (3.19)$$

The second term on the right-hand side of eq 3.18 involves all parameters of the radical system because of the convolution integral with  $f_a'(t) = P_{\text{eq}}[R]/T_1 + 2k_t[R]^2 P_F P_{\text{eq}}$ . However, if  $2|\omega_1| > |1/T_1 - 1/T_2|$ , the first term leads to transient nutations, which are determined only by the four parameters  $\omega_1$ ,  $T_1$ ,  $T_2$ , and  $M_Z(0)$ . Recently, Savitsky and Paul<sup>19</sup> showed that Fourier transformation of the transient nutations allows the determination of these four parameters with good accuracy from position, amplitude, and width of the nutation line in frequency space, and the line width at sufficiently late times after the radical generation.

If the radical relaxation rates are comparable with the initial exchange frequency, that is,  $T_{1,2}k_{\text{ex}}[R]_0 \geq 1$ , the effective relaxation times defined by eq 3.13 become time-dependent because of the chemical kinetics. Then, eqs 3.18 and 3.19 are no longer valid, and the Torrey oscillations have to be described by  $v(t)$  as calculated by integrating numerically the generalized Bloch equations (3.10–3.12), involving all parameters of the system simultaneously. Fortunately, a computer simulation shows that, also in the presence of exchange, good estimates for  $\omega_1$ ,  $M_Z(0)$ , the relaxation rate  $\sigma_0 = (T_1 + T_2)/2T_1T_2$ , and even the exchange rate  $k_{\text{ex}}[R]_0$  are still obtainable in a variety of cases from a simple analysis of the Torrey oscillations at different initial radical concentrations  $[R]_0$ .

For radical systems that carry only a multiplet-type polarization ( $M_Z^{\text{tot}} = P_{\text{eq}}[R]$ ), the exchange essentially only increases the relaxation rates, thus leading to a faster damping of the nutations. As an example, Figure 1i gives a comparison of two EPR-time profiles, which are calculated with  $k_{\text{ex}} = 0$  and  $k_{\text{ex}} = 2 \cdot 2k_t$ , respectively, all other parameters being the same (50 mW microwave power and  $T_2 = 2 \mu\text{s}$ ,  $T_1 = 4 \mu\text{s}$ ,  $2k_t = 2 \cdot 10^9 \text{ M}^{-1} \cdot \text{s}^{-1}$ ,  $P_F = -20$ ,  $P_m = 20$ ,  $[R]_0 = 10^{-4} \text{ M}$ ,  $\omega_1 = 5 \cdot 10^5 \text{ rad} \cdot \text{s}^{-1} / \text{mW}$ ,  $P_{\text{eq}} = 1 \text{ M}^{-1}$ , corresponding to  $\sigma_0 = 3.75 \cdot 10^5 \text{ s}^{-1}$ , and  $M_Z(0) = 2 \cdot 10^{-3}$ ). The Fourier transforms of both profiles are shown in Figure 1ii. Obviously, the exchange mainly broadens the nutation line and reduces its amplitude. The Lorentzian line shape is approximately maintained, as demonstrated by the broken line, which simulates the exchange-broadened nutation line on the basis of an assumed time dependence

$$v(t) = A \cdot e^{-\sigma t} \cdot \sin \omega_T t \quad (3.20)$$

With decreasing initial radical concentration the exchange rate becomes slower and the parameters  $A$ ,  $\sigma$ , and  $\omega_T$  of relation 3.20 approach  $M_Z(0)$ ,  $\sigma_0$ , and  $\omega_T \approx \omega_1$  according to eq 3.18.

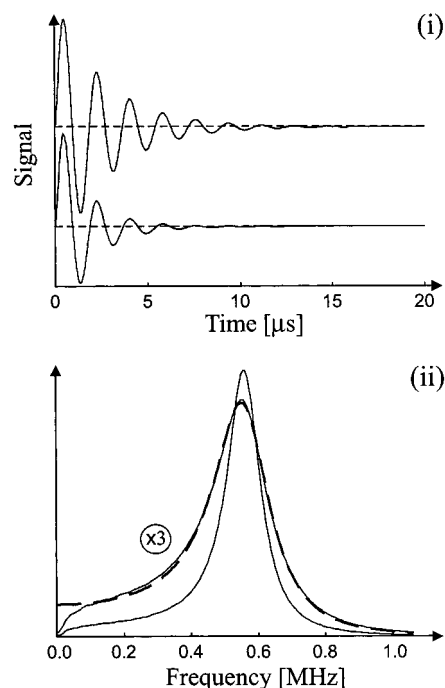


**Figure 1.** (i) EPR-time profiles calculated from eqs 3.10–3.12 for 50 mW microwave power and  $k_{\text{ex}} = 0$  (upper trace),  $k_{\text{ex}} = 2 \cdot 2k_t$  (lower trace), all other parameters (see text) being the same. (ii) Fourier transforms of the EPR-time profiles (i) and a simulation of the exchange broadened nutation line with eq 3.20, yielding  $\sigma = 6.23 \cdot 10^5 \text{ s}^{-1}$ ,  $\omega_T = 4.994 \cdot 10^5 \text{ rad} \cdot \text{s}^{-1} / \text{mW}$ , and  $A = 1.86 \cdot 10^{-3}$ .

Therefore, the latter parameters are obtainable from the variation of  $A$ ,  $\sigma$ , and  $\omega_T$  with the initial radical concentration  $[R]_0$ , which can be easily changed with the laser intensity in the time-resolved EPR experiment.  $\omega_1$  and  $\sigma_0$  are extractable by plotting  $\omega_T$  and  $\sigma$  versus  $A$  and extrapolating linearly to  $A = 0$ , and  $M_Z(0)$  is directly given by  $A$  at low laser intensities.

Even  $k_{\text{ex}}$  can be estimated if the initial radical concentration is known. For second-order radical termination reactions rate law 3.11 leads to the time dependence

$$[R](t) = [R]_0(1 + t/\tau)^{-1} \quad (3.21)$$

with  $1/\tau = 2k_t[R]_0$  being the second-order decay rate. As long as  $t/\tau \ll 1$  the radical concentration remains essentially constant, and the damping of the nutations is determined by  $\sigma = \sigma_0 + k_{\text{ex}}[R]_0$ . Thus,  $k_{\text{ex}}$  is just the initial slope in a plot of  $\sigma$  versus  $[R]_0$ , provided the termination rate is slow in comparison with the damping rate. Our simulations showed that this condition is sufficiently well fulfilled if the initial rate of damping,  $\sigma = \sigma_0 + k_{\text{ex}}[R]_0$ , is at least about four times faster than the initial rate of termination,  $2k_t[R]_0$ .

#### 4. Results

Upon UV irradiation of AIBN in solution, a steady-state EPR spectrum, which is composed of 21 first-order line groups, displayed in Figure 2i, is observed. It is unambiguously assignable to the 2-cyano-2-propyl radical because of the hyperfine couplings  $6\text{H}(\text{CH}_3)$ , 2.065 mT and  $\text{N}(\text{CN})$ , 0.336 mT, as well as the  $g$ -value 2.0030, which agree with reported data.<sup>20</sup> The TREPR spectra in Figure 2ii show the marked EPR lines of the  $(\text{CH}_3)_2\dot{\text{C}}\text{CN}$  radical [ $M_I(\text{H}) = -3 \dots 3$ ,  $M_I(\text{N}) = 0$ ], taken after certain time delays after the laser flash photolysis of AIBN. The lines are partially split into second-order components. Because AIBN decays from the singlet state, the resonances in

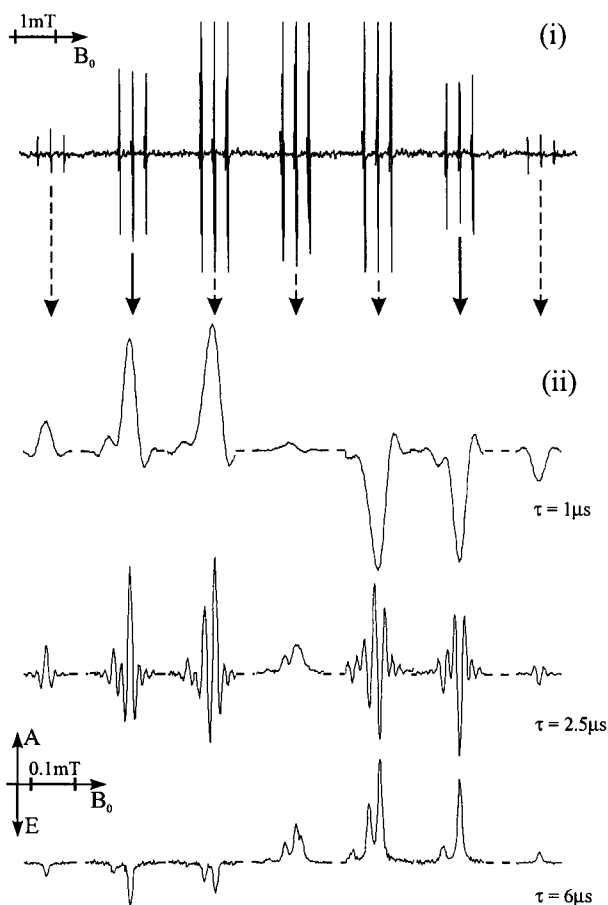


**Figure 2.** (i) Steady-state EPR spectrum of 2-cyano-2-propyl radicals obtained during continuous UV irradiation of AIBN in benzene solution. (ii) Sections of TREPR spectra taken at certain time delays after laser excitation of the same solution.

Figure 2ii exhibit an A/E pattern at short times due to the CIDEP from the geminate radical pairs. At later times, the F-pair polarization dominates and results in a phase inversion to an E/A multiplet. No initial net polarization is observed, indicating that either the photodissociation into  $N_2$  and two alkyl radicals is a concerted process, or the primary diazenyl radical  $\cdot NNC(CN)(CH_3)_2$ , if at all formed, decomposes into  $N_2$  and  $\cdot C(CN)(CH_3)_2$  in the picosecond range. This finding is in line with previous CIDNP results on the photolysis of symmetric azoalkanes.<sup>1</sup>

Two full arrows in Figure 2 mark a high- and low-field line [ $I(H) = 2$ ,  $M_I(H) = \pm 2$ ,  $M_I(N) = 0$ ], positioned symmetrically to the center of the spectrum. Their overlap with neighboring resonances is negligibly weak and, therefore, their EPR-time profiles have been chosen to investigate the CIDEP of the radical system. The time profiles on-resonance of these two lines were analyzed in terms of the modified Bloch equations discussed in the preceding section. For the AIBN system they consist of eqs 3.12–3.14 with additional use of eqs 3.10 and 3.21 for the total  $z$ -magnetization and the radical concentration. The initial conditions are defined by eqs 3.15–3.17, with  $P_n = 0$  and  $P_m = \pm P_G$  (geminate polarization) for the low- and high-field lines. Thus, the EPR-time profiles are governed by nine parameters in all, namely  $P_F$ ,  $P_G$ ,  $T_1$ ,  $T_2$ ,  $P_{eq}$ ,  $\omega_1$ ,  $k_{ex}$ ,  $2k_t$ ,  $[R]_0$ .

Five of these parameters were fixed via separate experiments, and the remaining ones were determined by least-squares fits of the equations to the profiles. First, the equilibrium polarization  $P_{eq}$  in signal units was measured by sensitivity calibrations of the spectrometer, using solutions of the persistent TEMPO

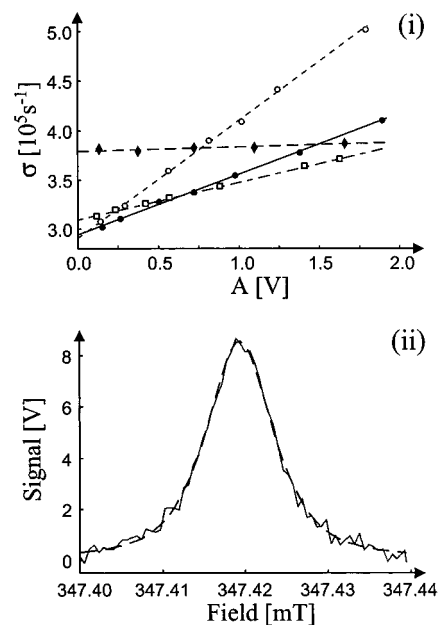


**Figure 3.** (i) Dependence of  $\sigma$  on  $A$  obtained from Torrey oscillations for:  $\circ$ , mix A, 2.09 cP;  $\bullet$ , mix B, 4.74 cP;  $\square$ , mix II, 9.27 cP;  $\blacklozenge$ , dibutyl phthalate, 17.73 cP. (ii) High-field line of 2-cyano-2-propyl radicals in benzene obtained by integration of the TREPR spectrum from 40 to 60  $\mu s$ , and its simulation by a Lorentzian with  $\Delta B_{1/2} = 9.2 \mu T$  (broken line).

radical in known concentration. Of course, the statistical weight of  $x_i/x = 5/192$  for the TREPR lines under investigation was accounted for. Details of the calibration procedure have already been described elsewhere.<sup>19</sup> Further, the EPR-time profiles of the two marked lines of the 2-cyano-2-propyl radicals were recorded at various laser intensities in the nutation limit (high microwave power). For each laser intensity at least four pairs of these time profiles were taken to evaluate amplitude  $A$ , damping  $\sigma$ , and nutation frequency  $\omega_T$  from the nutation line in frequency space, as described in the preceding section. Extrapolation to low initial radical concentrations then yielded  $M_Z(0) = P_G P_{eq} [R]_0$ ,  $\sigma_0 = (T_1 + T_2)/2T_1T_2$ , and the averaged microwave field amplitude  $\omega_1$  in the cavity. At times  $t \geq 40 \mu s$ , where the radical concentration is sufficiently low to make the exchange broadening negligibly small, the two EPR lines under investigation showed Lorentzian line shapes with a dependence on the incident microwave power following

$$\Delta B_{1/2}^2 = (\Delta B_{1/2}^0)^2 (1 + \omega_1^2 T_1 T_2) \quad (4.1)$$

with  $\Delta B_{1/2}^0 = 2/(\gamma T_2)$ . Therefore, the line width  $\Delta B_{1/2}$  at times  $t \geq 40 \mu s$  was determined at various microwave powers, and the relaxation times were calculated separately from  $2s_0 = 1/T_1 + 1/T_2$  and

$$1/2\sigma_0 \Delta B_{1/2}^2 \gamma^2 T_2^3 - (1/4\Delta B_{1/2}^2 \gamma^2 + \omega_1^2) \cdot T_2^2 - 2\sigma_0 T_2 + 1 = 0 \quad (4.2)$$

Some examples for these analyses are given in Figure 3. The dependence of  $\sigma$  on  $A$  for some solvents are shown in part i of the figure. The increasing influence of the spin exchange with decreasing viscosity of the solvent is clearly visible. The intercepts at  $A = 0$  yielded the values of  $\sigma_0$  for the various solutions. The quality of the line width measurement is demonstrated in Figure 3ii, which shows the high-field line of 2-cyano-2-propyl radicals in benzene (obtained by integrating the TREPR spectrum from 40 to 60  $\mu s$ ) and its simulation by

**TABLE 1: Parameter Set Obtained for 2-Cyano-2-propyl Radicals in a Variety of Solvents**

solvent	$\eta$ (cP)	$D_R^a$ ( $10^{-5}$ cm <sup>2</sup> s <sup>-1</sup> )	$2k_t^b$ ( $10^9$ M <sup>-1</sup> s <sup>-1</sup> )	$T_2$ ( $\mu$ s)	$T_1$ ( $\mu$ s)
benzene	0.66	1.93	2.1 (2.2)	$3.1 \pm 0.1$	$3.1 \pm 0.1$
ethyl benzoate	2.14	0.771	0.84 (1.0)	$2.55 \pm 0.3$	$5.1 \pm 0.5$
mix A <sup>c</sup>	2.09	—	0.84 (1.1)	$2.7 \pm 0.2$	$4.6 \pm 0.4$
mix I <sup>c</sup>	4.76	0.423	0.46 (0.6)	$2.6 \pm 0.2$	$4.9 \pm 0.4$
mix B <sup>c</sup>	4.74	—	0.46 (0.6)	$2.5 \pm 0.2$	$5.2 \pm 0.5$
mix II <sup>c</sup>	9.27	0.237	0.26 (0.4)	$2.4 \pm 0.3$	$4.7 \pm 0.4$
dibutyl phthalate	17.73	0.141	0.15 (0.2)	$1.95 \pm 0.1$	$4.15 \pm 0.3$

<sup>a</sup> Diffusion coefficient of 2-cyano-2-propane (as a model system for 2-cyano-2-propyl radical). <sup>b</sup> Values given in brackets are estimated from reported data.<sup>21</sup> <sup>c</sup> For mixture composition see the Experimental section.

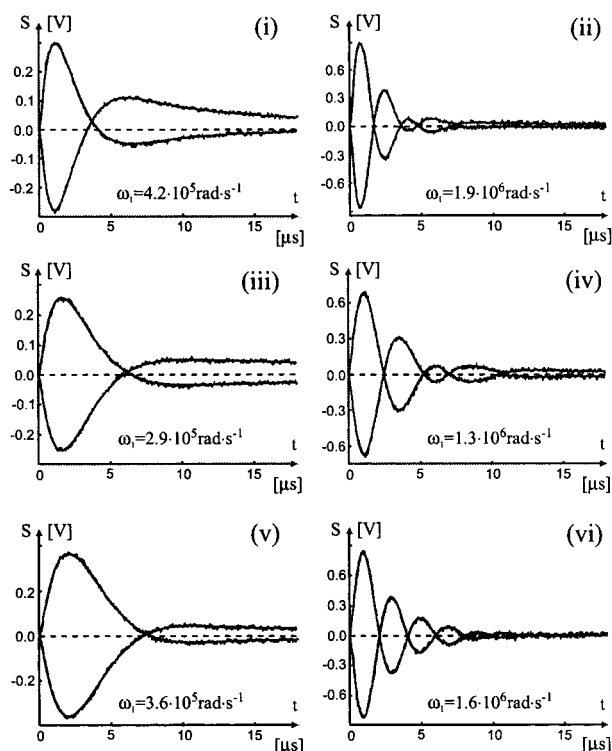


**Figure 4.** High- and low-field on-resonance EPR-time profiles of 2-cyano-2-propyl radicals after laser flash irradiation of AIBN, recorded at low and high microwave power in benzene (i, ii); in ethyl benzoate (iii, iv); in di-*n*-butyl phthalate (v, vi), as well as their simulations by eqs 3.12. The individual fits were obtained with  $\chi_{\text{red}}^2 \approx 1.5$ –1.7 at low power, and  $\chi_{\text{red}}^2 \approx 1.3$ –1.5 at high power, where the time dependence of the EPR signal is determined mainly by relaxation and  $\omega_1$ .

a Lorentzian with  $\Delta B_{1/2} = 9.2 \mu\text{T}$ . The relaxation times obtained for the 2-cyano-2-propyl radical in the various solutions are listed in Table 1.

The remaining four parameters  $[R]_0$ ,  $2k_t$ ,  $k_{\text{ex}}$ , and  $P_F$  were then determined by fitting with a SIMPLEX routine for each solvent the numerical solution of the Bloch equations to the EPR-time profiles of 15 high-/low-field resonance line pairs, which had been taken at various laser intensities and microwave powers. Two constraints were imposed in the analysis, namely a constant ratio of  $k_{\text{ex}}/2k_t$  for all solvents and a diffusion-controlled rate constant of radical termination, obeying  $2k_t \sim D$ . The latter condition has been proven in previous investigations,<sup>21</sup> and the former one corresponds to the assumption that the ratio of the cross-sections for exchange and termination is determined by the radicals and not the viscosity of the solvent.<sup>15,16</sup> Of course, the uniqueness of the fits were always checked by starting the SIMPLEX algorithm with different initial parameter sets. In addition, all fixed parameters were varied within their error limits, which did not improve the

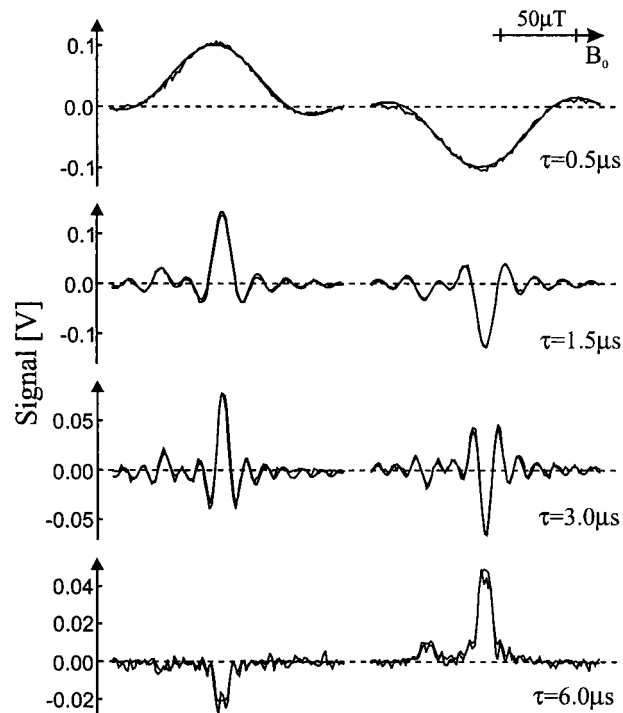


**Figure 5.** Experimental and calculated EPR lines of 2-cyano-2-propyl radicals ( $M_l(\text{H}) = \pm 2$ ) in benzene at different time delays after radical generation.

**TABLE 2: Polarization Factors  $P_G$  and  $P_F$  for the 2-Cyano-2-propyl EPR Lines with  $M_l(\text{H}) = \pm 2$ ,  $M_l(\text{N}) = 0$ , and In-cage Radical Termination Probability  $P_C$  in Different Solvents<sup>a</sup>**

solvent	$ P_G $	$ P_F $	$ P_F/P_G $	$P_C$
benzene	$18.7 \pm 0.8$	$19.3 \pm 1.8$	$1.03 \pm 0.04$	$0.67 \pm 0.05$
ethyl benzoate	$26 \pm 3$	$43 \pm 4$	$1.6 \pm 0.2$	$0.73 \pm 0.05$
mix A	$29 \pm 5$	$45 \pm 6$	$1.5 \pm 0.3$	—
mix I	$41 \pm 6$	$76 \pm 13$	$1.9 \pm 0.5$	$0.79 \pm 0.04$
mix B	$43 \pm 5$	$85 \pm 25$	$2.0 \pm 0.5$	—
mix II	$57 \pm 8$	$180 \pm 40$	$3.2 \pm 0.7$	$0.87 \pm 0.03$
dibutyl phthalate	$68 \pm 10$	$320 \pm 50$	$4.7 \pm 0.9$	$0.93 \pm 0.02$

<sup>a</sup> The polarization values are given in units of the equilibrium population difference  $p_{\text{eq}} = 7.8 \cdot 10^{-4}$ .

reduced  $\chi^2$ . Examples for the quality of the fits at low and high microwave powers are given in Figure 4 for three different solvents. Figure 5 demonstrates the congruence of the experimental and calculated resonance lines at different times after the laser flash. All results of the analyses are compiled in Tables 1 and 2. Table 2 also contains values for the in-cage termination probability  $P_C$  of the radicals. They were determined from the consumption per laser flash of the starting compound AIBN (measured by optical absorption spectroscopy before and after the TREPR experiment) and the initial radical concentration resulting from the fitting procedure.

In addition to the data given in the tables, the fit procedure also yielded a value for the ratio of the rates of radical spin exchange and termination,  $k_{\text{ex}}/2k_t = 2.6 \pm 0.2$ . This result is very close to the exchange/termination ratios, which were determined previously by Bartels et al.<sup>16</sup> for 2-hydroxy-ethyl (2.5) and 2-hydroxy-2-propyl (3.3) radicals in water. Following their analysis, it means that for the 2-cyano-2-propyl radicals the cross-section for exchange exceeds that for radical termination by a factor of  $1.8 \pm 0.2$ . Finally, our rate constants for radical termination agree well with the data given by Korth et al.<sup>21</sup> (see values given in brackets in Table 1), which further corroborates the reliability of the results of our multi-parameter analysis.

## 5. Discussion

The spin polarization and cage effect are both expected to depend on the initial spatial distance  $r_i$  of the radicals in the geminate pair. To discuss the data in Table 2, obtained after photolysis of AIBN, we will first supply the relations, which allow calculation of the CIDEP and cage effect in dependence on the initial separation of the species. Afterward some classical models for estimation of  $r_i$  will be summarized and their predictions compared with the experimental results.

**Diffusion Theory of CIDEP.** CIDEP is generated in radical pairs (RPs) during the free relative diffusion of the species. Geminate RPs start their diffusional trajectories after a fast primary separation process, which can result in an initial spatial distribution

$$\rho_2(r_i) = \frac{1}{4\pi r_i^2} \cdot \delta(r - r_i), \quad (5.1)$$

where  $r_i$  is the initial distance of both radicals. In the model of spherically symmetric species, the CIDEP generated in such a geminate RP can be found analytically by a method developed in ref 18. In particular, in the initial distribution (eq 5.1) this method yields the following expression for the multiplet CIDEP:

$$P_c^G(Q) = -2\text{Tr} \left\{ S_a \cdot \frac{1}{1 + \hat{\Lambda}\hat{k}} \cdot \frac{\hat{\Lambda}}{r_i} \cdot \exp[-\hat{k}(r_i - L_c)] \rho_0 \right\}, \quad (5.2)$$

for  $r_i \geq L_c$

Here  $\hat{\Lambda} = L_c - \hat{L}$ ,  $\rho_0 = |S\rangle\langle S|$  is the initial spin density matrix of the RP which is assumed to be singlet,  $\hat{k} = \sqrt{i\hat{H}_0/D}$ , and

$$\hat{H}_0 = \begin{pmatrix} 0 & Q & -Q & 0 \\ Q & 0 & 0 & -Q \\ -Q & 0 & 0 & Q \\ 0 & -Q & Q & 0 \end{pmatrix} \quad (5.3)$$

is the spin Hamiltonian of the free radicals (in  $ST_0$  approximation) in Liouville representation.<sup>22</sup> In the Hamiltonian (eq 5.3) the coupling

$$Q = 1/2 \left( \sum_j A_j^a I_{j_z}^a - \sum_k A_k^b I_{k_z}^b \right) \quad (5.4)$$

is expressed in terms of the difference of frequencies of the EPR lines of two radicals with hyperfine constants  $A_\nu^v$  ( $\nu = a, b$ ) in particular nuclear configurations. The supermatrix

$$\hat{L} = \begin{pmatrix} L_{SS} & 0 & 0 & 0 \\ 0 & L_{ST_0} & 0 & 0 \\ 0 & 0 & L_{T_0S} & 0 \\ 0 & 0 & 0 & L_{T_0T_0} \end{pmatrix} \quad (5.5)$$

characterizes the effect of reactivity and electron spin exchange interaction. This supermatrix is diagonal in the  $ST_0$ -basis and is composed of the effective reaction and spin exchange relaxation radii. For highly reactive species, that is, radicals which terminate diffusion controlled,

$$L_{SS} \sim d, L_{T_0T_0} = 0 \quad (5.6)$$

and

$$L_{ST_0} = L_{T_0S}^* = \begin{cases} d + \alpha^{-1} \left[ \ln \left( \frac{2J_0}{D\alpha^2} \right) + 1.16 \right] - i \cdot \frac{\pi}{2\alpha} \cdot \text{sign}(J), & 2J_0 > \pi/2D\alpha^2 \\ d - i\alpha^{-1} \cdot \frac{2J_0}{D\alpha^2}, & 2J_0 < \pi/2D\alpha^2 \end{cases} \quad (5.7)$$

where  $d$  is the distance of closest approach,  $D$  is the diffusion coefficient, and  $J_0$  and  $\alpha$  characterize the distance dependence of the exchange interaction,  $J(r) = J_0 \cdot \exp[-\alpha(r - d)]$ . The parameter  $L_c$  is defined by the relation

$$L_c = \text{Re}(L_{ST_0}) = \begin{cases} d + \alpha^{-1} \left[ \ln \left( \frac{2J_0}{D\alpha^2} \right) + 1.16 \right], & 2J_0 > \pi/2D\alpha^2 \\ d, & 2J_0 < \pi/2D\alpha^2 \end{cases} \quad (5.8)$$

In the same approximation the probability  $P_d^G(Q)$  of escape from geminate recombination and, correspondingly, the recombination probability  $P_r^G(Q)$  are given by

$$P_d^G(Q) = 1 - P_r^G(Q) = \text{Tr} \left\{ \hat{\Pi}(r_i) \rho_0 + \frac{1}{1 + \hat{\Lambda}\hat{k}} \cdot \frac{\hat{\Lambda}}{r_i} \cdot \exp[-\hat{k}(r_i - L_c)] \rho_0 \right\} \quad (5.9)$$

where  $\hat{\Pi}(r_i) = 1 - \hat{L}/r_i$  is the supermatrix of escaping probabilities in the absence of any quantum evolution of the free radicals, that is, for  $\hat{H}_0 = 0$ .

Expressions similar to eqs 5.2 and 5.9 can be derived for the rate  $K_c$  of CIDEP generation and the rate  $K_r$  of recombination in the bulk process<sup>23</sup>:

$$K_c = 2\pi D L_c P_c^F \quad \text{and} \quad K_r = 2\pi D L_c P_r^F \quad (5.10)$$

where  $P_c^F$  is the CIDEP amplitude that is given by eq 5.2 for  $r_i = L_c$  and the uncorrelated initial condition  $\rho_0 = (|S\rangle\langle S| + |T_0\rangle\langle T_0|)/2$ , and  $P_r^F = 1 - P_d^F$  is the recombination probability with  $P_d^F$  given by eq 5.9 for the same  $r_i$  and  $\rho_0$ .

All observable  $P_c(Q)$  and  $P_d(Q)$  should be averaged over nuclear configurations, that is, over all  $Q$ -values, taking into account, however, that in averaging  $P_c(Q)$ , some of them, which do not correspond to the observed component of hyperfine multiplet of the investigated radical, should be omitted. For

convenience, the values  $P_\nu$  averaged over  $Q$  are denoted

$$\bar{P}_\nu = \langle P_\nu(Q) \rangle_Q \quad (5.11)$$

In terms of these notations the CIDEP per radical escaping geminate recombination and the CIDEP per radical undergoing F-pair recombination are expressed by

$$p_e^G = \bar{P}_e^G / \bar{P}_d^G \quad \text{and} \quad p_e^F = \bar{P}_e^F / \bar{P}_r^F \quad (5.12)$$

respectively. In what follows, the viscosity (diffusion coefficient) dependence will be discussed and compared with the experiment of the cage effect

$$P_c(D) = 1 - \bar{P}_d^G \quad (5.13)$$

and the ratio of F- and G-pair polarization,

$$R_c(D) = P_F(D)/P_G(D) = \bar{P}_e^F / \bar{P}_e^G \quad (5.14)$$

The exponential term in eqs 5.2 and 5.9 gives rise to the important effect of loss of spin coherence in the RP in the case of a large initial distance  $r_i$  between the species. This loss shows itself in a substantial change of the CIDEP when

$$\varphi = \|\hat{k}(r_i - L_e)\| \sim \sqrt{Q/D} \cdot (r_i - L_e) \quad (5.15)$$

changes from  $\varphi < 1$  to  $\varphi > 1$  as a function of  $r_i$ . If  $\varphi < 1$  then  $\exp[-\hat{k}(r_i - L_e)] \approx 1$  and the effect of  $r_i$  is essentially absent except for the trivial  $1/r_i$  dependence, which results in a slow change of the CIDEP with change of  $r_i$ . However, if  $\varphi > 1$  then the CIDEP of singlet RPS can even change signs, when the RP spin density matrix has almost completely relaxed to that of F-pairs at the moment of the first re-encounter.<sup>22</sup>

The most common mechanical models for estimation of  $r_i$  will be outlined in the following text, and the free diffusion model will be applied to the dependence on  $D$  of the geminate recombination probability and the CIDEP. It is evident from eqs 5.2 and 5.9 and the discussion above that this dependence is determined mainly by that of  $\varphi$ , which results not only from the relation  $\varphi \sim D^{-1/2}$  but also from the dependence  $r_i(D)$ .

**Primary Spatial Separation and Comparison with Experiment.** The process of geminate recombination of RPs in homogeneous liquids starts with the initial spatial separation of the radicals, which is followed by spin/space evolution and partial recombination during subsequent diffusive re-encounters. The characteristic time of the primary separation stage is fairly short ( $\sim 10^{-11} - 10^{-13}$  s) and corresponds to the time resolution of optical and IR spectroscopic measurements.<sup>6-8,24,25</sup> The time of separation is typically much shorter than the times of spin evolution and the times that can be investigated in TREPR experiments. This stage, however, is important for the description of the cage effect and the geminate pair CIDEP because it essentially determines the initial condition for the magnetic field dependent spin/space evolution of the RPs.

The most popular model of primary separation assumes that after formation the radicals move apart from each other because of the initial translational energy resulting from the impulse of a repulsive force.<sup>26,27</sup> After dissipation of this initial energy the radicals undergo a relative diffusive motion from the distance  $\bar{r}_i$  which can be estimated, according to Noyes,<sup>26</sup> within the simple Langevin approach as

$$\Delta r = \bar{r}_i - d \approx \frac{v_0}{\gamma_r} = \left( \frac{v_0 m}{kT} \right) D \quad (5.16)$$

where  $v_0$  is the initial relative velocity of the radicals,  $\gamma_r$  is the velocity relaxation rate,  $D$  is the relative diffusion coefficient, and  $m$  is the mass of the radicals. Applying Stokes law

$$D = \frac{kT}{3\pi d\eta} \quad (5.17)$$

one obtains the corresponding viscosity dependence of  $\bar{r}_i$ .

Relations 5.16 and 5.17 are obtained in the simplified Langevin approximation which is valid for macroscopic particles and is not very accurate when applied to small molecules. However, the same formula (eq 5.16) can also be derived in the more realistic generalized Langevin approach,<sup>28</sup> which accounts for the memory effects in the energy dissipation process in liquids. Despite such an essential generalization the Langevin approach is still approximate because it treats solvents as homogeneous liquids and thus does not describe the local inhomogeneity of liquids at small distances of the order of molecular sizes. In other words, eq 5.16 can be used only for qualitative analysis of the process.

In addition to Noyes' formula (eq 5.16), which predicts the relation  $\Delta r \sim D$ , another dependence,

$$\Delta r \sim \sqrt{D} \quad (5.18)$$

also can be considered as physically reasonable. This relation implies a diffusion-like primary separation. In reality it corresponds to the following scenario of the process. During the dissociation the energy excess of the process gives rise to a local heating of the surrounding molecules and, thus, to a higher mobility of these molecules and a high diffusion coefficient  $D^*$ , which is, nevertheless, proportional to the initial diffusion coefficient  $D$ . During the time of fast cooling the radicals will diffuse apart from each other to an average distance  $\Delta r \approx (D^* \tau^*)^{1/2}$ , where  $\tau^*$  is the characteristic temperature relaxation time of the heated surrounding molecules to the lower macroscopic temperature of the liquid. In principle,  $\tau^*$  can change with viscosity so that the viscosity dependence of  $\Delta r$ , that is, the dependence on  $D$ , can be complicated. However, in liquids, the heat transfer and thus  $\tau^*$  is controlled by processes (typically VV-transfer) completely different and almost independent of those that determine the viscosity and mass transfer. This means that the time  $\tau^*$  is expected to change only weakly with viscosity. In such a case, the initial separation dependence on  $D$  is given by eq 5.18. The main drawback of this model is the same as that of the Noyes model: it does not take into account the local inhomogeneity at molecular distances and the eventual caging due to short-range interactions between the radicals.

Finally, the loss of  $N_2$  in the dissociation process of azoalkanes also must be considered. The nitrogen molecule may act as some kind of spacer between the radicals. If this governed the initial distance  $r_i$  one would expect it as essentially independent of viscosity, that is,

$$\Delta r = \text{constant} \quad (5.19)$$

For comparison with the experimental results, it is convenient to use dimensionless quantities  $x$  for the distance and  $q$  for the inverse diffusion coefficient (viscosity), defined by

$$x = r/d \quad \text{and} \quad q = Ad^2/D \sim 1/D \sim \eta \quad (5.20)$$

In further evaluations a distance of closest approach of  $d = 6$  Å and a characteristic hyperfine constant of  $A = 2$  mT were chosen for the radical pairs being formed by photolysis of AIBN.



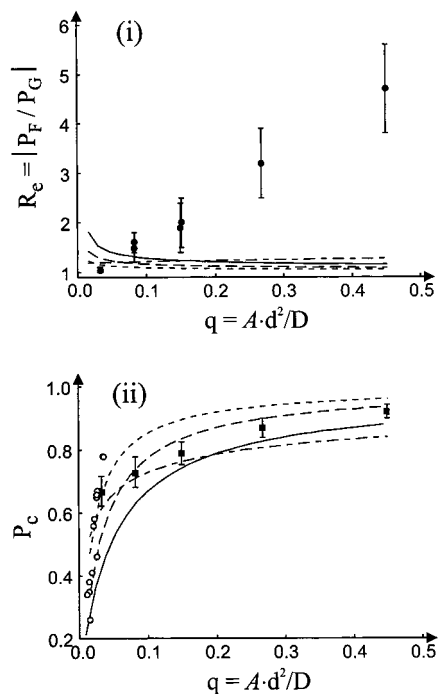


**Figure 6.** Comparison of the experimental  $q$ -dependences of the polarization ratio  $R_e(q)$  (i) and cage effect  $P_C(q)$  (ii) with theoretical predictions calculated within the free diffusion model for (—)  $\Delta x(q) = \Delta r/d = 0.025/q$ ; (---)  $\Delta x(q) = 0.015/q$ ; (— · —)  $\Delta x(q) = 0.04/q$ ; and (— · — · —)  $\Delta x(q) = 0.10/\sqrt{q}$ .  $L_{SS} = d$  (diffusion-controlled recombination) and  $J_0/A = 155$  were taken for all calculations. ■, Data from Table 2; ○, reported data.<sup>10,29–33</sup>

The three dependences  $\Delta x(q) = \Delta r(q)/d$  discussed above can be combined in the expression:

$$\Delta r(q)/d = \delta + \lambda_1/\sqrt{q} + \lambda_2/q \quad (5.21)$$

The Noyes and diffusion models of the primary separation correspond to  $\delta = \lambda_1 = 0$  and  $\delta = \lambda_2 = 0$ , respectively, whereas a constant initial separation, independent of  $q$ , means  $\delta \neq 0$ ,  $\lambda_1 = \lambda_2 = 0$ .

As for the other parameters used for the calculation of the polarization ratio  $R_e$  and the in-cage reaction probability  $P_C$  in dependence on  $q$ :

1. The exchange interaction was assumed to be not very strong:  $J_0/A = 155$  (i.e.,  $J_0 \approx 0.31$  T), so that in the considered range of diffusion coefficients  $D = 10^{-6} - 10^{-4}$  cm<sup>2</sup>·s<sup>-1</sup> there exists the transition from the case  $2J_0 < (\pi/2)Da^2$  to the opposite case  $2J_0 > (\pi/2)Da^2$ , which shows itself in a rather sharp change of the slope of the function  $P_e^G(q)$ . The exchange interaction dependent parameters have been calculated from formulas 5.7 and 5.8 with  $\alpha = 5/d$ . Although these formulas are approximate, they reproduce the exact behavior of the CIDEP, including the above-mentioned sharp change of the slope of  $p_e(q)$ , quite accurately.<sup>18,28</sup>

2. The reactivity of the radicals was assumed to be high, so that the effective radius of recombination in the singlet state is of the order of  $d$ :  $L_{SS} \sim d$ . However, a possible reaction probability  $< 1$  for singlet RPs at distance  $d$ , that is,  $L_{SS} < d$  has also been considered.

Figure 6 shows the experimental (see Table 2 and reported data<sup>10,29–33</sup> for  $P_C$ ) and theoretical dependences  $P_C(q)$  and  $R_e(q)$  for  $D$ -dependent initial distances  $r_i$  calculated from eq 5.21 with  $\delta = 0$ ,  $\lambda_2 = 0$  (the dependence  $\Delta r \sim \sqrt{D} \sim 1/\sqrt{q}$ ) and  $\delta = 0$ ,  $\lambda_1 = 0$  (the dependence  $\Delta r \sim D \sim 1/q$ ), respectively.

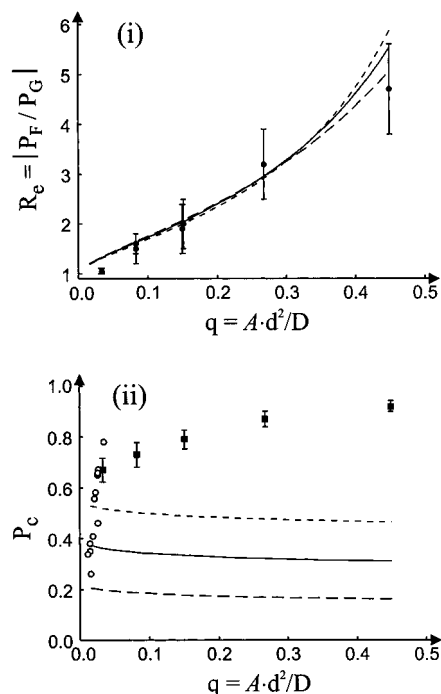


**Figure 7.** Same as Figure 6 but for  $\Delta x(q) = \Delta r(q)/d$  independent of  $q$ : (—)  $\Delta x = 1.2$ ,  $L_{SS}/d = 0.5$ ; (—)  $\Delta x = 1$ ,  $L_{SS}/d = 0.8$ ; (---)  $\Delta x = 0.8$ ,  $L_{SS}/d = 1$ .

Obviously, the dependence  $\Delta r \sim D$  and  $\Delta r \sim \sqrt{D}$  enables one to obtain a good agreement between theory and experiment for  $P_C(q)$ . However, the behavior of the CIDEP dependence  $R_e(q)$  is predicted in complete contradiction with the experimental one.

The same functions  $P_C(q)$  and  $R_e(q)$  but for  $r_i$  independent of  $q$  ( $\lambda_1 = \lambda_2 = 0$ ) are displayed in Figure 7. It is seen that the discrepancy is now reversed. For reasonable values of  $r_i$  ( $r_i - d \approx$  one molecular diameter) the experimentally obtained dependence of the ratio of F- and geminate pair CIDEP,  $R_e(q)$ , can be reproduced quite well. At the same time, the agreement for the cage effect  $P_C(q)$  is inadequate: the theoretical dependence on  $q$  is too weak, is decreasing with  $q$ , and has a lower absolute value as compared with the experimental one.

Of course one can find compromises by setting all three parameters in eq 5.21 unequal zero, but any pronounced decrease of  $r_i$  with increasing viscosity, as is needed to describe the cage effect, weakens the change of  $R_e$  with  $q$  toward unity. Unambiguously, for the 2-cyano-2-propyl radical pairs formed by photocleavage of AIBN the classic Langevin models for the initial separation  $r_i$  are unable to simultaneously describe the viscosity dependence of the cage effect and the CIDEP. At present, the reason for this discrepancy is not quite clear. As mentioned before, the total cage effect is composed of a primary (reaction during the fast separation stage) and secondary (diffusive return from  $r_i$  to  $d$ ) one, and  $P_C(q)$ , of course, represents the  $q$ -dependence of the sum of both. But at least at low viscosities (low  $q$ -values), the primary cage-effect cannot be dominant, because most radicals are escaping the cage, so that at low viscosities the secondary cage effect should be a major part of  $P_C$  and, therefore, be reflected in  $P_C(q)$ . However, this is obviously not the case. Because the CIDEP data are rather directly connected with  $r_i$ , it has to be concluded that, at least for the photocleavage of AIBN, the successful simulation of the viscosity-dependent cage effect on the basis of a decreasing initial radical separation with increasing viscosity is only fortuitous. Studies of other compounds will have to show if this finding is limited to the AIBN system or a more general feature.

**Acknowledgment.** The authors thank Dr. Judith Geimer and Prof. Dieter Beckert from Leipzig University for some control experiments with FT-EPR and the Swiss National Foundation for Scientific Research for financial support of this work, which is also part of the INTAS project 99-01766. A. I. S. acknowledges a grant from the Russian Foundation for Fundamental Research.

### References and Notes

- (1) Engel, P. S. *Chem. Rev.* **1980**, *80*, 99; and references therein.
- (2) Buback, M.; Huckestein, B.; Kuchta, F.-D.; Russell, G. T.; Schmid, E. *Macromol. Chem. Phys.* **1994**, *195*, 2117; and references therein.
- (3) Salikhov, K. M.; Molin, Yu. N.; Sagdeev, R. Z.; Buchachenko, A. L. *Spin Polarization and Magnetic Effects in Radical Reactions*; Elsevier: New York, 1984; and references therein.
- (4) Adrian, F. J. *Rev. Chem. Intermed.* **1986**, *7*, 173; and references therein.
- (5) Nagakura, N.; Hayashi, H.; Azumi, T. *Dynamic Spin Chemistry*; Kodansha: Tokyo, 1998; and references therein.
- (6) Harris, A. L.; Brown, J. K.; Harris, C. B. *Annu. Rev. Phys. Chem.* **1988**, *39*, 341; and references therein.
- (7) Schroeder, J.; Troe, J. *Annu. Rev. Phys. Chem.* **1987**, *38*, 163; and references therein.
- (8) Schwartz, B. J.; King, J. C.; Zhang, J. Z.; Harris, C. B. *Chem. Phys. Lett.* **1993**, *203*, 503.
- (9) Jent, F.; Paul, H. *Chem. Phys. Lett.* **1989**, *160*, 632.
- (10) Jaffe, A. B.; Skinner, K. J.; McBride, J. M. *J. Am. Chem. Soc.* **1972**, *94*, 8510; and references therein.
- (11) Zytowski, T.; Fischer, H. *J. Am. Chem. Soc.* **1997**, *119*, 12869.
- (12) Rügge, D.; Fischer, H. *J. Chem. Soc., Faraday Trans. 1* **1988**, *84*, 3187.
- (13) (a) Lipscher, J. Ph.D. Thesis, Universität Zürich, 1982. (b) Okamoto, K.; Hirota, N.; Terazima, M. *J. Phys. Chem.* **1997**, *101*, 5380 have argued that transient radicals diffuse somewhat more slowly than the diamagnetic parent compounds. Even if that is true, it would affect our analysis only marginally.
- (14) Molin, Yu. N.; Salikhov, K. M.; Zamarayev, K. I. *Spin Exchange*; Springer-Verlag: Berlin, 1980.
- (15) Syage, J. A.; Lawler, R. G.; Trifunac, A. D. *J. Chem. Phys.* **1982**, *77*, 4774.
- (16) Bartels, D. M.; Trifunac, A. D.; Lawler, R. G. *Chem. Phys. Lett.* **1988**, *152*, 109.
- (17) Pedersen, J. B. *J. Chem. Phys.* **1973**, *59*, 2656.
- (18) Shushin, A. I. *Chem. Phys.* **1990**, *144*, 201, 223.
- (19) Savitsky, A. N.; Paul, H. *Appl. Magn. Res.* **1997**, *12*, 449.
- (20) Landolt-Börnstein *Magnetic Properties of Free Radicals, New Series*, Group II, Vol. 9b; Fischer, H., Hellwege, K.-H., Eds.; Springer: Berlin, 1977.
- (21) Korth, H.-G.; Lommers, P.; Sicking, W.; Sustmann, R. *Int. J. Chem. Kinet.* **1983**, *15*, 267.
- (22) Shushin, A. I.; Pedersen, J. B.; Lolle, L. I. *Chem. Phys.* **1993**, *177*, 119.
- (23) Hanngi, P.; Talkner, P. *Rev. Mod. Phys.* **1990**, *62*, 251; and references therein.
- (24) Haan, S. W. *Phys. Rev. A* **1979**, *20*, 2516.
- (25) Saven, J. G.; Skinner, J. L. *J. Chem. Phys.* **1993**, *99*, 4391.
- (26) Noyes, R. M. *Prog. React. Kinet.* **1961**, *1*, 129.
- (27) Otto, B.; Schroeder, J.; Troe, J. *J. Chem. Phys.* **1984**, *81*, 202.
- (28) Shushin, A. I. *Chem. Phys. Lett.* **1987**, *133*, 562.
- (29) Walling, C.; Kurkov, P. *J. Am. Chem. Soc.* **1967**, *89*, 4895.
- (30) Burkhart, R. D. *J. Phys. Chem.* **1966**, *70*, 605.
- (31) Bartlett, P. D.; Funahashi, T. *J. Am. Chem. Soc.* **1962**, *84*, 2596.
- (32) Hammond, G. S.; Senn, J. N.; Boozer, C. E. *J. Am. Chem. Soc.* **1955**, *77*, 3244.
- (33) Burkhart, R. D.; Merrill, J. C. *J. Phys. Chem.* **1969**, *73*, 2699.